Talanta 85 (2011) 1063–1069

Contents lists available at ScienceDirect

Talanta

journal homepage: www.elsevier.com/locate/talanta

Determination of arsenic based on quenching of CdS quantum dots fluorescence using the gas-diffusion flow injection method

Nutthaya Butwong, Tuanjai Noipa, Rodjana Burakham, Supalax Srijaranai, Wittaya Ngeontae*

Department of Chemistry and Center for Innovation in Chemistry, Faculty of Science, Khon Kaen University, Khon Kaen 40002, Thailand

ARTICLE INFO

Article history:
Received 30 January 2011
Received in revised form 10 May 2011
Accepted 12 May 2011
Available online 19 May 2011

Keywords:
Arsenic
Fluorescence quenching
Quantum dots
Gas diffusion unit

ABSTRACT

A sequential injection analysis system for determination of arsenic based on hydride generation and fluorescence quenching of mercaptoacetic acid capped cadmium sulfide quantum dots (CdS–MAA QDs) is described. The generated arsine diffused across the PTFE membrane in a gas-diffusion unit and subsequently interacted with CdS–MAA QDs. The parameters affecting the arsine generation and the fluorescence quenching of QDs were studied. Under the optimum conditions, it was observed that a increase in the concentration of As(III) corresponded well to a decrease in fluorescence intensity according to the Stern–Volmer relationship. The extent of quenching was dependent on the concentration of arsenic in the range of 0.08–3.20 mmol L^{-1}, with the detection limit of 0.07 mg L^{-1}. The precision (%RSD) from eight replicates of the determination of As(III) 1.0 mg L^{-1} was found to be 1.4%. The proposed method was applied to the determination of arsenic in ground water samples with satisfactory recoveries.

1. Introduction

Arsenic has been recognized as one of the most toxic elements [1]. Several analytical methods have been developed to detect arsenic in various sample matrices. Atomic absorption spectrometry (AAS) is the most frequently used method which involves the reduction of arsenic to arsine and then detection as the hydride in a quartz cell. Although this approach is very sensitive and selective, it uses expensive instrumentation with high operating cost. Analytical techniques based on spectrophotometry, including UV-visible [2] and spectrofluorometry [3], have been successfully applied for determination of arsenic. Automated flow injection (FI) techniques coupled to spectrophotometry have also been used [4]. In addition, the selectivity of the FI methods has been improved by the introduction of an online gas-diffusion unit (GDU) [5,6].

Another method which provides sensitivity comparable to AAS is chemiluminescence (CL) detection. Inorganic arsenic species have been successfully determined in batch and FI systems using luminol-based chemiluminescence detection [7–9]. However, fluorescent dyes have some limitations including instability, broad emission spectra and low signal intensities.

During the past two decades, quantum dots (QDs) have gained considerable attention in chemistry. QDs are widely used as fluorescence probes or sensors [10–19]. For analytical application, the surface of QDs needs to be modified by stabilizing agents such as L-cysteine and mercaptoacetic acid (MAA) [10–13]. It has been reported that the types of the stabilizing agents influence the optical and chemical properties of QDs on the surface [16]. During the last few years, there have been many reports on the application of CdS QDs as the fluorescence probe for determination small molecules and ions based on the fluorescence quenching strategy [11,12,14,15]. For example, Chen and Zhu [10] investigated L-cysteine capped CdS QDs as a luminescence probe for heavy and transition metal (HTM) ions in aqueous solution. They found that the photophysics of the fluorescence emission from the functionalized CdS QDs was significantly influenced by Ag(I). Koneswaran and Narayanaswamy [11] demonstrated that Hg(II) can quenched MAA capped CdS QDs. This method can be used to detect the mercury ion at nanomolar levels with no interference from other serious coexisting cations. Wu and Zhao [13] applied MAA capped CdS QDs for the determination of hydrogen selenide ions (HSe^- ions), at micromolar to sub-micromolar levels. Recently, Wang et al. [19] reported a novel fluorescence spectrometric method for the determination of As(III) at ultra trace level by using glutathione capped CdTe QDs. As(III) has a high-affinity to interact with glutathione capped CdTe QDs whereas MAA capped CdTe or CdTe/ZnS QDs have no response to As(III). However, the determination of arsenic based on quenching fluorescence intensity measurements of CdS–MAA QDs has not yet been reported. Since it has been reported that As(III) and AsH_3 can interact with –SH group and S–S bond [20–23], the interaction of AsH_3 and MAA capped CdS QDs was expected.

This work is aimed at developing a new method for arsenic determination based on the fluorescence quenching of MAA capped CdS quantum dots. The online arsine generation was carried out

* Corresponding author. Tel.: +66 432 02222x12243; fax: +66 432 02373.
E-mail address: wittayange@kku.ac.th (W. Ngeontae).

0039-9140/$ – see front matter © 2011 Elsevier B.V. All rights reserved.
doi:10.1016/j.talanta.2011.05.023

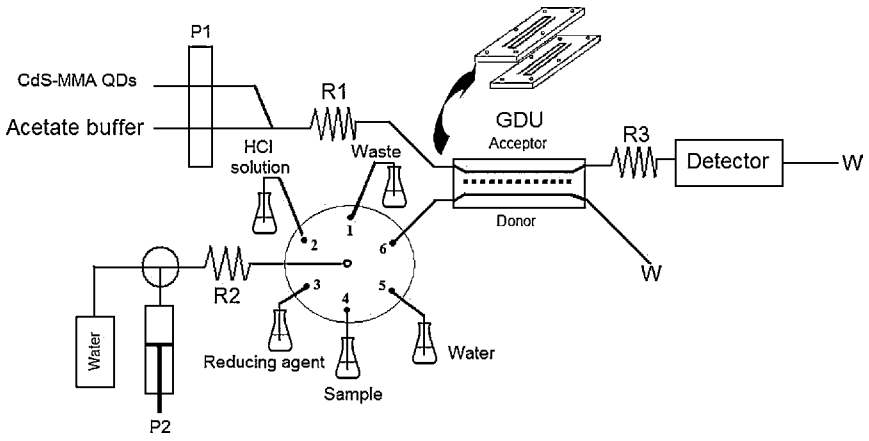

Fig. 1. Schematic diagram of the on-line gas diffusion system.

using a sequential injection analysis (SIA) system coupled with GDU. Then, the generated arsine diffused through PTFE membrane to the CdS–MAA QDs stream and caused the fluorescence quenching. The concentration of arsenic was related to the quenching efficiency of the fluorescence intensity. The validation and application of the purposed method was investigated in water samples.

2. Experimental

2.1. Reagents

All reagents were of analytical-reagent grade and used without further purification. All aqueous solutions were prepared with deionized water with a resistivity of 18.2 MΩ cm (Millipore, France). Cadmium chloride ($CdCl_2{\cdot}H_2O$) was purchased from Riedel-de Haën (German). Mercaptoacetic acid (MAA) was obtained from Sigma Aldrich (USA). Sodium sulfide ($Na_2S{\cdot}9H_2O$) was obtained from BDH (England). Sodium borohydride ($NaBH_4$) and As(III) stock solution (1000 mg L^{-1}) were obtained from Fluka (USA). Standard solutions of As(III) were made up daily by appropriate dilution of the As(III) stock solution with 0.5 mol L^{-1} HCl solution. The As(III) stock solution was kept in a sealed container in a refrigerator at 4 °C when not in use. The AAS standard solutions (1000 mg L^{-1}) of all metal ions and other reagents were purchased from Carlo Erba (France). The acetate buffer solution was made from 0.1 mol L^{-1} acetic acid/sodium acetate and adjusted to appropriate pH by 1.0 mol L^{-1} NaOH against the pH meter.

2.2. Instrumentation

The flow system (Fig. 1) consisted of a 10-port VICI® multiposition valves (Valco instruments Co. Inc., USA), a Cavro® syringe pump (Tecan Group Ltd., Switzerland) and a Watson Marlow 505S peristaltic pump (Watson Marlow, USA). The GDU consisted of two rectangular Perspex blocks (15.0 cm length, 5.0 cm width and 1.5 cm height) held together by stainless steel screws. Each block was groove drilled (3 grooves, 100 mm length, 1 mm width and 1 mm depth for each groove) and they were separated by a PTFE membrane of 0.076 mm thickness.

The length of reaction coil (R2) was fixed at 500 cm to generate arsine and provide a controlled release of generated gas in the GDU. A reaction coil (R1, 100 cm) was used for mixing CdS–MAA solution and acetate buffer solution. The length of reaction coil (R3) was varied from 30 to 100 cm. All connecting lines and the reaction coils were made from 0.5 mm i.d. Teflon tubing.

A Shimadzu RF-5301pc spectrofluorometer (Shimadzu, Japan) was used for recording the fluorescence spectra. All fluorescence spectra were obtained at room temperature using a xenon lamp as the excitation source equipped with a 3.5-mL standard quartz cuvette (10 mm × 10 mm) or Shimadzu RF-540 flow cell unit. An Agilent 8453 UV-visible Spectrophotometer (Agilent, USA) equipped with a 1 cm quartz cell was used for recording the absorption spectra. IR spectroscopy was performed by a Perkin Elmer Spectrum GX FT-IR/FT-Raman spectrometer (Perkin Elmer, USA).

2.3. Procedure

2.3.1. Synthesis of mercaptoacetic acid capped CdS

Water-soluble CdS QDs capped by MAA were synthesized following the method reported by Winter et al. [24] with some modifications. $CdCl_2{\cdot}H_2O$ (3.7751 g, 18.75 mmol) was dissolved in 200 mL of water. Then, MAA (37.50 mmol) was added into the solution under stirring and the solution pH was adjusted to 10.5 with 1 mol L^{-1} NaOH solution. After that, 10 mL of the aqueous solution containing 1.4632 g of $Na_2S{\cdot}9H_2O$ (18.75 mmol) was quickly added to the Cd^{2+} solution with vigorous stirring and the solution gradually turned yellow. The reaction mixture was stirred at 65 °C for 60 min and then aged at room temperature in air for 3 h without stirring.

2.3.2. Hydride generation gas diffusion flow system

The arsine was generated by the reaction in Eq. (1). Using the online gas diffusion system (Fig. 1), the aspiration flow rate of sample, HCl, and $NaBH_4$ solution were set at 50 μL min^{-1}. Aliquots of the HCl (2 × 50 μL), sample or standard solution of arsenic (3 × 100 μL) and $NaBH_4$ (2 × 200 μL) were sequentially aspirated into the holding coil (R2) through ports 2, 4 and 3, respectively. The aspiration sequence was HCl/As(III)/$NaBH_4$/As(III)/$NaBH_4$/As(III)/HCl and the generated AsH_3 was propelled to donor channel of the GDU through port 6 at a flow rate of 20 μL min^{-1}. Generated arsine diffused through the PTFE membrane and interacted with CdS–MAA QDs in 10 mmol L^{-1} acetate buffer (acceptor stream). The analyte was preconcentrated by the stopped-flow time of the acceptor stream for 90 s. The acceptor was then delivered to the fluorescence detector at a flow rate of 0.5 mL min^{-1} through a 50-cm reaction coil (R3).

$$As(OH)_3 + 3BH_4^- + 3H^+ \rightarrow AsH_3 + 3BH_3 + 3H_2O \quad (1)$$

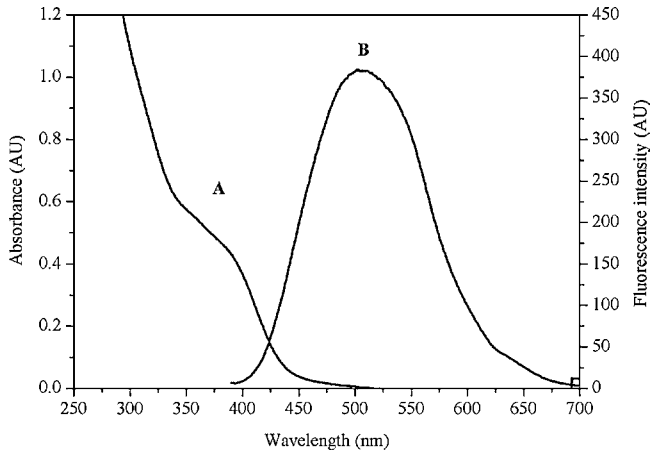

Fig. 2. Absorption (A) and room temperature fluorescence spectra (B) of CdS–MAA QDs.

3. Results and discussion

3.1. Characteristics of CdS–MAA QDs

The optical properties of CdS–MAA QDs were studied using the UV-visible spectrophotometer and spectrofluorometer. The absorption spectrum of CdS–MAA QDs is shown in Fig. 2(A), with a weak shoulder at around 375 nm. From the position of the absorption edge, the average particles size can be estimated using the well-established relation between particles size and absorption onset [24–26]. The absorption edge (λ_e) is converted into the corresponding particle size using Henglein's empirical curve that relates λ_e to the diameter (2R) of the particles as shown in Eq. (2).

$$2R_{CdS} = \frac{0.1}{(0.138 - 0.0002345\lambda_e)\ \text{nm}} \quad (2)$$

From Fig. 2(A) the absorption edge (λ_e) was obtained by the intersection of the sharply decreasing region of the spectrum with the baseline and found to be 450 nm. Based on the absorption onset of the synthesized CdS–MAA, the average diameter is ~3.1 nm, calculated using Henglein's empirical curve which has been widely used to calculate the particle size of CdS QDs capped by thiol molecule [26]. Using Peng's empirical curve [27], the average diameter was calculated to be ~5.3 nm. However, Peng's empirical was derived using a difference type of ligand and different synthesis methods. TEM image (Fig. 3) showed a high distribution of particle size and provided larger particle size estimates than those from the three-dimensional confinement models mentioned above. Since the average particle size of QDs in this work is out of the ranges that cover by both approaches neither model is appropriate for estimating the particle size of QDs in this study [27].

The fluorescence characteristics of the synthesized QDs were also investigated by exciting at 375 nm. The CdS–MAA QDs emitted the fluorescence with symmetrical spectrum showing the maximum intensity at 510 nm (Fig. 2(B)). The full width at half-maximum (FWHM) of CdS–MAA QDs was ≈120 nm with the quantum yield of ≈1.23% which corresponded to the particle size dispersion of the synthesized QDs [28]. Moreover, the CdS–MAA QDs were also characterized by FT-IR spectroscopy. From IR spectra (Fig. 4), peaks for carboxyl and carbonyl groups on the surface of the CdS–MAA QDs were observed. The IR spectra showed the significant peaks at 1567, 1387, and 1228 cm^{-1} and loss of peaks at around 2572 cm^{-1} which confirmed that the MAA was functionalized on the surface of CdS QDs [11,29]. In addition, peaks were observed at wavenumbers 500–700 cm^{-1}, indicating the presence of Cd–S bond [24,26].

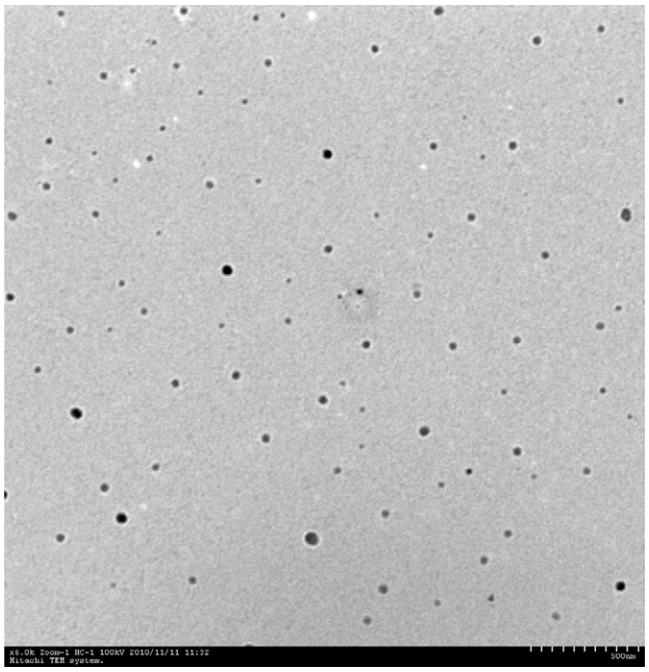

Fig. 3. TEM image of CdS–MAA QDs. 500-nm scale bar.

From the above evidence, it can be concluded that CdS–MAA QDs was successfully synthesized. The CdS–MAA QDs were stable in the dark under ambient conditions for at least a month without obvious.

3.2. Effect of CdS–MAA QDs concentration on fluorescence intensity

The concentration of CdS–MAA QDs was optimized for the determination of arsenic. The fluorescence intensity increased dramatically with the increase in the CdS–MAA QDs concentration, with the maximum concentration of 5.0 mM. It decreased at higher concentrations (data not shown). The decreased fluorescence intensity at higher concentrations may be due to self-quenching of fluorescence of the CdS–MAA QDs [11].

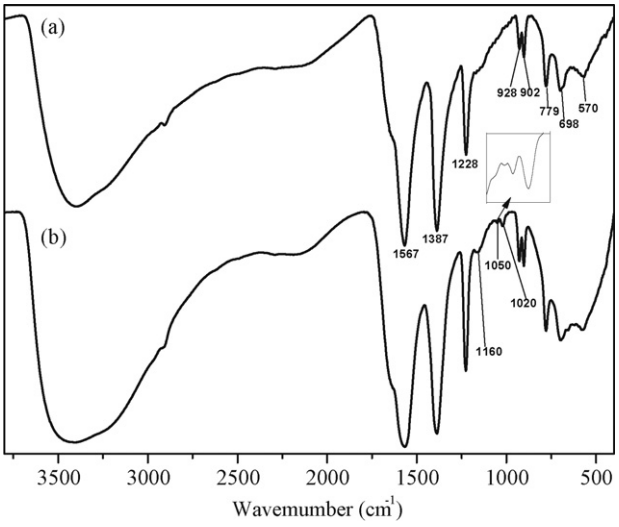

Fig. 4. The FT–IR absorption spectra of CdS–MAA before (a) and after (b) interaction with arsine.

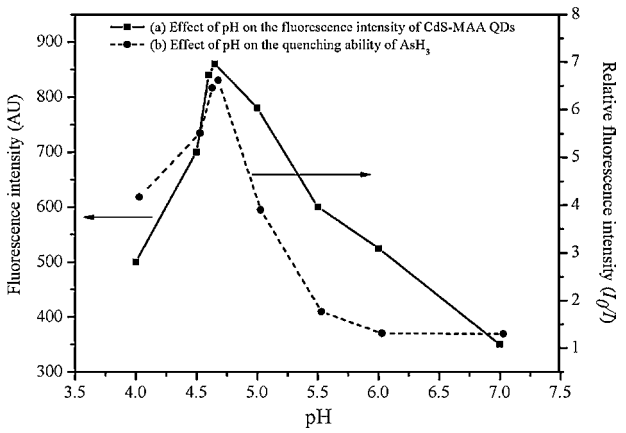

Fig. 5. Effect of pH on the fluorescence intensity and I_0/I; λ_{em} = 510 nm (λ_{ex} = 375 nm). 1.87 mmol L^{-1} of CdS–MAA QDs and 1.0 mg L^{-1} of arsenic.

3.3. Effect of pH on luminescence of CdS–MAA QDs

The influence of pH on the fluorescence of CdS–MAA QDs was studied and the results are shown in Fig. 5(a). The maximum fluorescence intensity was observed at pH 4.6, resulting from the strong interaction between QDs and MAA [30]. Higher pHs (pH > 4.6) provided lower intensities which may be due to the formation of hydrated products and decreased solubility of QDs [11–13]. Lower pHs (pH < 4.6) also showed lower fluorescence intensities, indicating the precipitation of CdS nanocrystal. In acidic medium, the detachment of the ligand (MAA) from the QDs has been reported [30,31]. As noted in Fig. 5(a), pH is a critical parameter affecting fluorescence intensity, so different buffers were then studied to control pH of the QDs solution. Acetate buffer provided higher fluorescence intensity compared to phosphate buffer and did not affect the fluorescence intensity of CdS–MAA QDs. Therefore, acetate buffer (10 mmol L^{-1}) was chosen for further studies.

In addition, it was found that the solution pH also affect to the quenching ability of CdS–MAA QDs fluorescence intensity by AsH_3. The solution pH was studied and the results were evaluated in terms of the relative fluorescence intensity (I_0/I). It can be seen in Fig. 5(b) that at pH 4.6 the I_0/I was the highest, indicating the maximum quenching by AsH_3. Therefore, pH 4.6 was chosen for further experiments.

3.4. Effect of arsine on the fluorescence intensity of CdS–MAA QDs

The fluorescence spectra of CdS–MAA QDs were studied in the semi-batch system. The arsenic concentration was varied from 0.1 to 8.0 mg L^{-1}. The acceptor stream (CdS–MAA QDs) was separated from the donor stream (arsenic, HCl and $NaBH_4$) by the PTFE membrane. Arsenic was converted into arsine by mixing with the $NaBH_4$ solution in the holding coil (R2) before passing to the GDU. After the generated arsine passed through the PTFE membrane and interacted with CdS–MAA QDs stream, the mixing solution zone was then delivered into detector and the fluorescence spectrum was recorded.

Fig. 6 depicts the absorption and fluorescence emission spectra of CdS–MAA QDs in the absence and presence of arsine at difference concentrations of arsenic. A decrease in fluorescence intensity of the CdS–MAA QDs solution was observed when there was interaction with arsine. The fluorescence intensity and absorbance of CdS–MAA QDs gradually decreased with increasing concentrations of arsenic. In addition, it is clearly seen that the fluorescence band centered at 510 nm (excitation 375 nm) and the absorption spectra did not shift with increasing concentration of arsenic. When the arsenic concentration was increased to 8 mg L^{-1}, the CdS–MAA QDs fluorescence was completely diminished. Considering the significant quenching of fluorescence intensity, this observation suggests the possibility of developing a sensitive method for determination of arsenic based on the quenching of CdS–MAA QDs.

3.5. Online determination of arsenic

The experimental parameters affecting the hydride generation were optimized to achieve high sensitivity, good precision and high sample throughput. For the system shown in Fig. 1, the system parameters (concentrations of HCl, $NaBH_4$, CdS–MAA QDs and acetate buffer) were optimized. Furthermore, the dispensing flow rate, sample volume and stopped-flow time were also investigated. The working ranges within these parameters were varied, along with the corresponding optimal values are presented in Table 1.

3.5.1. Hydride generation (donor stream)

The optimization of the donor stream was intended to achieve high yield arsine generation and to ensure that most of the generated arsine could pass through the PTFE membrane to the acceptor stream. The studied parameters were the concentration of HCl and $NaBH_4$, the dispending flow rate, the sample volume. The aspiration flow rates of all reagents were set to be identical at 50 μL min^{-1}. The length of holding coil (R2) was fixed at 500 cm and provide a controlled release of generated gas in the GDU. While varying the parameters of the donor stream, the conditions used with the acceptor stream were fixed as follows: CdS–MAA QDs 2.0 mmol L^{-1} dissolved in acetic–acetate buffer 10 mmol L^{-1} with a delivery flow rate of 0.5 mL min^{-1}. It was observed that when the generated arsine passed through PTFE membrane to the acceptor stream, some waiting time was required to ensure interaction with CdS–MAA QDs. From this reason, the solution flow was stopped for various time intervals and it was found that 1 min after the arsine zone arrived to the GDU was optimal. The optimum value of each parameter describe above was chosen based on the maximum quenching efficiency and signal intensity are summarized in Table 1.

The mixing order of the solution can affect the efficiency of the arsine generation [32]. Four patterns of the flow segmentation were investigated (in Table 1). The results showed that the aspiration sequence of HCl/As(III)/BH_4^-/As(III)/BH_4^-/As(III)/HCl provided the maximum yield of arsine, as indicated by the maximum quenching of the fluorescence.

The dispensing flow rate of the donor stream was another important parameter in the on-line gas-diffusion analyses that was varied, since it determines the contact time between the arsine and the semi-permeable membrane and, therefore, the efficiency of the diffusion process. It was found that when the flow rate decreased from 60 to 10 μL min^{-1}, the relative fluorescence intensity (I_0/I) increased more than 300% (data not shown). In order to compromise between sensitivity, peak broadening and sample throughput, the flow rate of 20 μL min^{-1} was chosen.

The influence of the sample volume was studied in the range of 90–600 μL. Using the aspiration pattern number 4, (HCl/As(III)/BH_4^-/As(III)/BH_4^-/As(III)/HCl), the I_0/I sharply increased with the sample volume up to 300 μL. However, the increase in the I_0/I ratios were not related to the sample volumes higher than 300 μL. Therefore, the sample volume of 300 μL (100 μL × 3) was selected.

The effects of $NaBH_4$ and HCl concentrations were also studied as shown in Fig. 7. The HCl concentration was varied over the range of 0.3–0.9 mol L^{-1}. The signal increased with the increasing of HCl concentrations from 0.3 to 0.5 mol L^{-1}, while leveling-off occurred thereafter. Thus, 0.5 mol L^{-1} was selected. In addition, the volume of HCl was studied in the range of 100–300 μL, and peak heights were

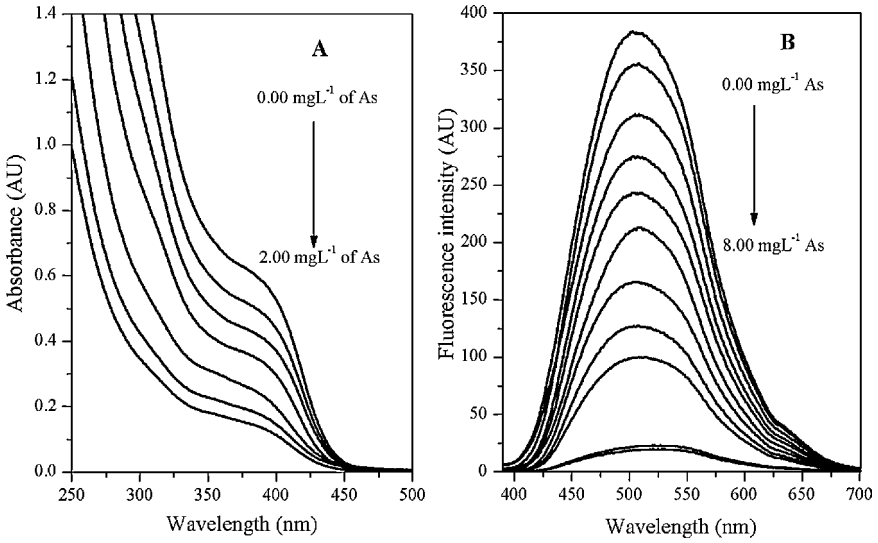

Fig. 6. Absorption (A) and fluorescence emission (B) spectra of CdS–MAA QDs in the absence and presence of different concentrations of arsenic (arsine) pH 4.63; λ_{em} = 510 nm (λ_{ex} = 375 nm) 0.2 mmol L^{-1} CdS–MAA QDs.

found to be virtually unaffected in the studied range. Therefore, 200 μL (2 × 100) was chosen since it provided sufficient acidity.

The concentration of $NaBH_4$ was studied from 0.3 to 0.9% (*w*/*v*). The I_0/I slightly decreased with higher concentrations of $NaBH_4$ (0.6–0.9, % *w*/*v*). This may be due to the generation of hydrogen gas bubbles which have the solubility in aqueous media higher than arsine and are able to diffuse through the PTFE membrane and mix with the CdS–MAA solution. Thus, the interaction between arsine and CdS–MAA should decrease. The hydrogen generation during hydride generation has been reported by others [5,33]. Therefore, the value of $NaBH_4$ 0.5% (*w*/*v*) was chosen for further studies.

In addition, increasing the total volume of $NaBH_4$ from 100 to 400 μL resulted in an increase in the I_0/I ratio. However, the I_0/I ratio gradually decreased when the volume increased to 600 μL. Therefore, 400 μL (2 × 200 μL) of $NaBH_4$ was chosen.

3.5.2. Acceptor stream

The parameters affect the fluorescence intensity of CdS–MAA QDs were investigated using the optimum condition obtained from Section 3.5.1. The studied parameters were the solution pH and the buffer concentration. The concentration of the acetate buffer was varied from 5 to 30 mmol L^{-1} and it was found that 10 mmol L^{-1} acetate buffer (pH 4.63) provided the maximum signal.

Moreover, the time required for the arsine to pass through PTFE membrane was also investigated in terms of the stopped-flow time of the acceptor stream when the arsine zone reached the membrane. The contact time can enhance arsine mass transfer towards the membrane in the donor stream and compensate for the dispersion effect in the acceptor stream. The results revealed that the signal obtained from the system by controlling the stopped-flow time of the acceptor stream was considerably higher than those obtained from the configuration with continuous acceptor stream. The stopped-flow time was then studied from 0 to 120 s. The results showed that the signal increased with increasing stopped-flow time up to 90 s and then the signal decreased when the stopped-flow time was longer than 90 s. This may result from zone broadening of the analyte due to the use of the stopped flow-time mode [34] or there may be more interference (hydrogen and its subsequent oxidation) from the donor stream passing through the membrane and interact with CdS–MAA QDs [33].

The interaction of arsine and CdS–MAA QDs was investigated by varying the length of the reaction coil (R3) in the range of 30–100 cm. The maximum signal was obtained at a length of 50 cm, thus this length was adopted for further experiments to provide the adequate mixing of the generated arsine and CdS–MAA solution.

Using the optimum conditions (as summarized in Table 1), the blank and standard As(III) were studied and the obtained signals are shown in Fig. 8. It is clearly seen that the fluorescence intensity decreased only in the presence of arsine, while there was no significant decrease in the fluorescence intensity in the blank solu-

Table 1
Optimization of the on-line hydride generation gas diffusion system.

System parameter	Range studied	Optimal value
Donor stream		
$NaBH_4$ concentration (%, *w*/*v*)	0.3–0.9	0.5
HCl concentration (mol L^{-1})	0.3–0.9	0.5
Flow rate (μL min^{-1})	10–60	20
Sample volume (μL)	90–600	300 (100 × 3)
Acceptor stream		
Concentration of CdS–MAA QDs (mmol L^{-1})	0.1–2.0	1.87
Concentration of acetate buffer pH 4.63 (mmol L^{-1})	5.0–30	10
Flow rate (mL min^{-1})	0.5–1.0	0.5
Stopped-flow time (s)	0–120	90
Aspiration pattern	(1) HCl/As(III)/BH_4^-/HCl (2) HCl/As(III)/BH_4^-/As(III)/BH_4^-/HCl (3) HCl/As(III)/BH_4^-/As(III)/HCl (4) HCl/As(III)/BH_4^-/As(III)/BH_4^-/As(III)/HCl	4
Reaction coil length; R3 (cm)	30–100	50

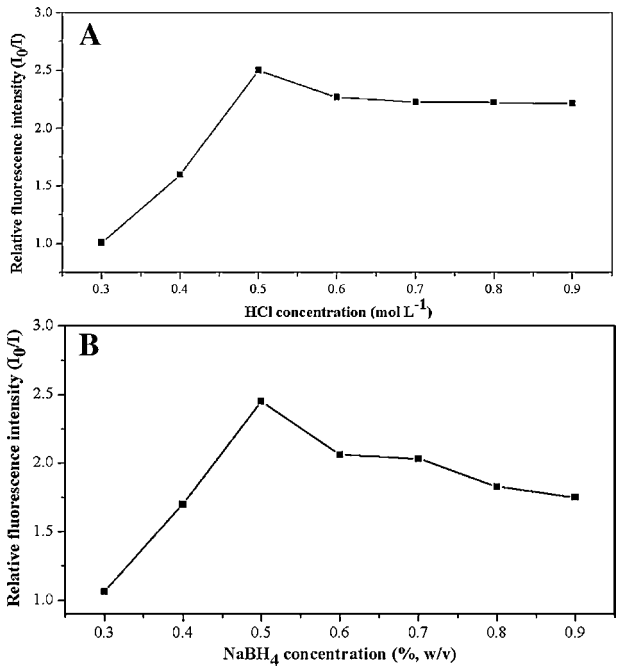

Fig. 7. Effect of HCl (A) and $NaBH_4$ (B) concentrations on the relative fluorescence intensity (I_0/I). (A) 0.5 mg L^{-1} As(III); [$NaBH_4$] = 0.5%(w/v). (B) 0.5 mg L^{-1} As(III); [HCl] = 0.5 mol L^{-1}.

tion (HCl and $NaBH_4$). These results indicate that the use of the PTFE membrane has eliminated the effect of ions which interfere in arsenic determination via arsine generation.

3.6. Possible interaction between CdS–MAA QDs and generated arsine

Several quenching mechanisms have been proposed to explain how metal ions quench the fluorescence of functionalized QDs: inner filter effect, non-radiative recombination pathway, electron transfer process and ion binding interaction [10–19]. Fig. 6 shows the absorption and fluorescence emission spectra of CdS–MAA QDs in the absence and presence of different concentrations of arsenic. According to the absorption and fluorescence emission spectra of QDs in the presence of arsine (Fig. 6), there was no significant shift of the full width at half-maximum (FWHM) of the fluorescence spectra and the absorption spectra when increasing the concentration

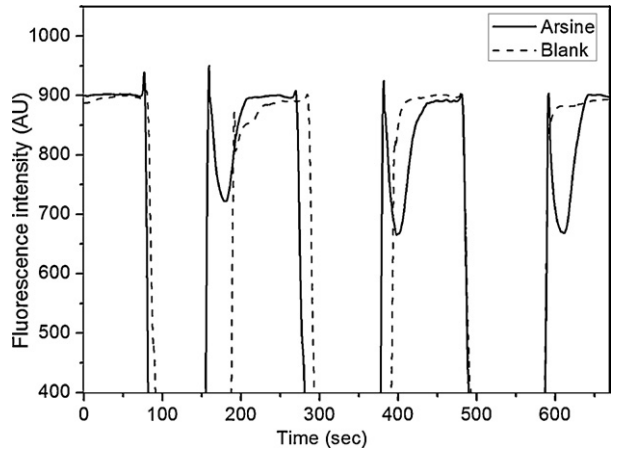

Fig. 8. Fluorescence signal obtained from the triplicate determination of 0.2 mg L^{-1} As(III) standards (solid line) and reagent blank (broken line) under the optimum conditions.

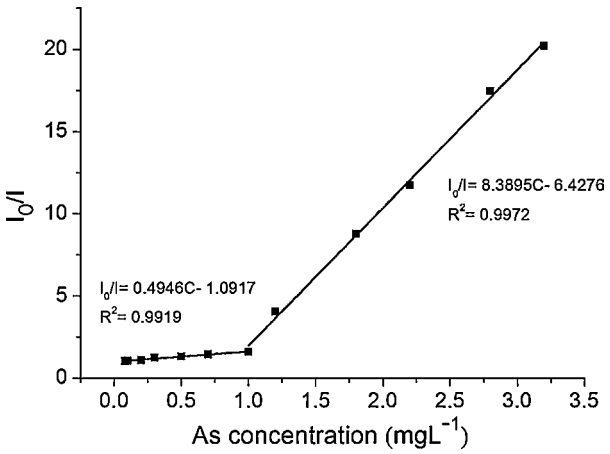

Fig. 9. Plot of the I_0/I value against arsenic concentration. Concentrations of arsenic used were 0.08, 0.10, 0.20, 0.30, 0.50, 0.60, 1.0, 1.20, 1.60, 2.20, 2.80 and 3.20 mg L^{-1}. Each point was averaged from at least three replicates, operated at ambient temperature.

of arsenic. It can be concluded that the quenching mechanism may occur only on the functionalized groups [13]. According to the IR spectra (Fig. 4) of the QDs after contact with the generated arsine, new peaks at 1160, 1050 and 1020 cm^{-1} were observed. Moreover, the relative peak intensities at around 500–800 cm^{-1} were changed from those of CdS–MAA QDs. This observation may due to the formation of new bonds on the functional group of QDs [35]. In addition, it has been known that arsine is a strong reducing agent and the ability of arsine to reduce the covalent bond was reported [20–23]. From the above evidences, the quenching of CdS–MAA QDs fluorescence intensity in this study may due to the formation of As–S on MAA functional group of CdS–MAA QDs surface.

3.7. Calibration and reproducibility

The Stern–Volmer equation [12], Eq. (3), was applied to investigate the relationship between quenching efficiency and concentration of quencher (i.e., As concentration)

$$\frac{I_0}{I} = K_{SV}C + 1 \quad (3)$$

I_0 and I are the fluorescence intensities in the absence and presence of arsine, respectively. Plotting I_0/I as a function of C yields a linear plot with a slope equal to K_{SV}. When varying the arsenic concentrations, the results obtained (Fig. 9) were well correlated with the Stern–Volmer equation in two linear ranges. Both ranges in which the fluorescence is not completely quenched yielded the following equations: $I_0/I = 0.4946C - 1.0917$ (C in mg L^{-1}) for 0.08–1.00 mg L^{-1} of As ($r^2 = 0.9919$) and $I_0/I = 8.3895C - 6.4276$ (C in mg L^{-1}) for 1.00–3.20 mg L^{-1} of As ($r^2 = 0.9972$). The two linear slopes are likely to be a result of different sizes of separate populations of QDs. This correlates well with the TEM of the synthesized QDs. Since the CdS–MAAs prepared in this work showed high variation in particle size distribution, the quenching efficiency may be different. The two linear working ranges this may be the resulted of different abilities of smaller and larger particles to interact with generate arsine [36]. The calibration curves of both concentration ranges are depicted in Fig. 9. The Stern–Volmer quenching constants (K_{SV}) were 3.76×10^4 and 6.32×10^5 M^{-1} for the lower and upper concentration ranges, respectively. The detection limit (LOD) was found to be 0.07 mg L^{-1} using the criterion of 3 times the standard deviation of the blank signal. The precision (%RSD) from eight replicates of the determination of 1.00 mg L^{-1} As(III) was 1.4%, indicating that the proposed method provided good sensitivity and good precision.

Table 2
Interference study.

Foreign ion	Tolerance limit (mg L^{-1})
SO_4^{2-}	500
NO_3^-	500
CO_3^{2-}	500
PO_4^{3-}	500
Cl^-	500
Br^-	500
I^-	500
Ni^{2+}	5.0
Cu^{2+}	5.0
Cd^{2+}	5.0
Fe^{3+}	5.0
Pb^{2+}	5.0
Hg^{2+}	0.5

Table 3
Percentage recovery of arsenic in synthetic sample.

Arsenic added (mg L^{-1})	Arsenic found (mg L^{-1})	Recovery (%)[a]
0.00	N.D.	N.D.
0.10	0.09	93 ± 2.0
0.50	0.49	95 ± 0.7
1.00	0.98	93 ± 1.7

N.D., not detected.
[a] Average ± S.D. (n = 3).

3.8. Interferences

The selectivity of the present method was evaluated by studying the influence of common anions and cations on the determination of arsenic in binary mixture system. The experiments were carried out by fixing the concentration of As(III) at 0.5 mg L^{-1} and then recording fluorescence intensity before (I_S) and after adding the foreign ion (I_{SF}). The tolerance level is defined as resulting relative error (%RE) = $(I_S - I_{SF})/I_{SF} \times 100$ less than ±5%. The results of interference studied are shown in Table 2. From the results, the common anions such as chloride, carbonate, nitrate, phosphate and sulfate did not interfere at concentrations up to 500 mg L^{-1}. The interference of transition metal ions was also investigated. It was found that Hg(II) gave significant negative bias when present at concentration equivalent to As(III). On the other hand, Fe(III), Ni(II), Cu(II), Pb(II) and Cd(II) could be present (<5% interference) at concentrations up to 5 mg L^{-1}.

3.9. Application to ground water sample

The feasibility of the proposed method was evaluated by total arsenic determination of ground water and spiked ground water samples. The samples were digested using concentrated HCl and heating at 90 °C for 30 min. The results showed that arsenic was not detected in all studied samples. However, accuracy was evaluated from recovery by spiking As(III) at different concentrations into the sample matrices. Percent recoveries were in the range of 93–95%, as summarized in Table 3, demonstrating good accuracy.

4. Conclusions

A detection method for As(III) based on the fluorescence quenching of CdS–MAA QDs after interaction with generated arsine via the automated flow system was successfully developed. The FI system was used for controlling the generation of arsine from As(III). The generated arsine diffuses through PTFE membrane in GDU to interact with CdS–MAA QDs in an acceptor stream which controlled the flow rate by FI and finally transport into a spectrofluorometer. The high selectivity of the assay against commonly reported interfering ions in arsenic determination is a result of the membrane based GDU separation and the specificity of the interaction between arsine and CdS–MAA. The detection limit of this proposed method was 0.07 mg L^{-1}. There were no serious interferences from common anions and other transition metal ions at low concentrations. The proposed method was applied to the determination of As(III) in spiked ground water samples with good recoveries (93–95%). In addition, this method is simple, automated and reliable for screening total arsenic in environmental samples.

Acknowledgements

This research was supported by the Higher Education Research Promotion and National Research University Project of Thailand, Office of the Higher Education Commission, through the Advanced Functional Materials Cluster of Khon Kaen University, the Rajamangala University of Technology Isan (RMUTI) and the Center for Innovation in Chemistry (PERCH-CIC), Commission on Higher Education, Ministry of Education. The authors are grateful for the helpful discussion from Prof. Richard L. Deming (Department of Chemistry and Biochemistry, California State University, Fullerton, CA).

References

[1] N.V. Semenova, F.M. Bauzá de Mirabó, R. Forteza, V. Cerdá, Anal. Chim. Acta 412 (2000) 169–175.
[2] S. Kundu, S.K. Ghosh, M. Mandal, T. Pal, A. Pal, Talanta 58 (2002) 935–942.
[3] S.R. Goode, R.J. Matthews, Anal. Chem. 50 (1978) 1608–1611.
[4] Z.-L. Fang, Anal. Chim. Acta 400 (1999) 233–247.
[5] T. Rupasinghe, T.J. Cardwell, R.W. Cattrall, M.D. Luque de Castro, S.D. Kolev, Anal. Chim. Acta 445 (2001) 229–238.
[6] C. Lomonte, M. Currell, R.J.S. Morrison, I.D. McKelvie, S.D. Kolev, Anal. Chim. Acta 583 (2007) 72–77.
[7] Y. Tamari, A. Takada, H. Tsuji, Y. Kusaka, Anal. Sci. 4 (1988) 277–280.
[8] M. Li, S.H. Lee, Microchem. J. 80 (2005) 237–240.
[9] S. Satienperakul, T.J. Cardwell, S.D. Kolev, C.E. Lenehan, N.W. Barnett, Anal. Chim. Acta 554 (2005) 25–30.
[10] J.L. Chen, C.Q. Zhu, Anal. Chim. Acta 546 (2005) 147–153.
[11] M. Koneswaran, R. Narayanaswamy, Sens. Actuators B 139 (2009) 91–96.
[12] M. Liu, L. Xu, W. Cheng, Y. Zeng, Z. Yan, Spectrochim. Acta Part A 70 (2008) 1198–1202.
[13] C.L. Wu, Y.B. Zhao, Anal. Bioanal. Chem. 388 (2007) 717–722.
[14] Y. Chen, Z. Rosenzweig, Anal. Chem. 74 (2002) 5132–5138.
[15] M.S. Mehata, H.B. Tripathi, J. Lumin. 99 (2002) 47–52.
[16] P. Jorge, M.A. Martins, T. Trindade, J.L. Santos, F. Farahi, Sensors 7 (2007) 3489–3534.
[17] A.-N. Liang, L. Wang, H.-Q. Chen, B.-B. Qian, B. Ling, J. Fu, Talanta 81 (2010) 438–443.
[18] Y. Long, D. Jiang, X. Zhu, J. Wang, F. Zhou, Anal. Chem. 81 (2009) 2652–2657.
[19] X. Wang, Y. Lv, X. Hou, Talanta 84 (2011) 382–386.
[20] L.T. Rael, F. Ayala-Fierro, R. Bar-Or, D.E. Carter, D.S. Barber, Toxicol. Sci. 90 (2006) 142–148.
[21] D.E. Carter, H.V. Aposhian, A.J. Gandolfi, Toxicol. Appl. Pharmacol. 193 (2003) 309–334.
[22] H.F. Gilbert, Adv. Enzymol. Relat. Areas Mol. Biol. 63 (1990) 169–172.
[23] H.F. Gilbert, Methods Enzymol. 251 (1995) 8–28.
[24] J.O. Winter, N. Gomez, S. Gatzert, C.E. Schmidt, B.A. Korgel, Colloids Surf. A 254 (2005) 147–157.
[25] R. He, X.F. Qian, J. Yin, H.A. Xi, L.J. Bian, Z.K. Zhu, Colloids Surf. A 220 (2003) 151–157.
[26] J. Chen, A. Zheng, Y. Gao, C. He, G. Wu, Y. Chen, X. Kai, C. Zhu, Spectrochim. Acta Part A 69 (2008) 1044–1052.
[27] W.W. Yu, L. Qu, W. Guo, X. Peng, Chem. Mater. 15 (2003) 2854–2860.
[28] C. de Mello Donegá, S.G. Hickey, S.F. Wuister, D. Vanmaekelbergh, A. Meijerink, J. Phys. Chem. B 107 (2003) 489–496.
[29] T. Awatani, A.J. McQuillan, J. Phys. Chem. B 102 (1998) 4110–4113.
[30] A. Mandal, N. Tamai, J. Phys. Chem. C 112 (2008) 8244–8250.
[31] C. Landes, C. Burda, M. Braun, M.A. El-Sayed, J. Phys. Chem. B 105 (2001) 2981–2986.
[32] B.E.R. Cordero, M.P. Cañizares-Macías, Talanta 78 (2009) 1069–1076.
[33] T.W.T. Rupasinghe, T.J. Cardwell, R.W. Cattrall, S.D. Kolev, Anal. Chim. Acta 652 (2009) 266–271.
[34] J.C. Vauthier, P.S. Williams, J. Chromatogr. A 805 (1998) 149–160.
[35] T.-L. Zhang, Y.-S. Xia, X.-L. Diao, C.-Q. Zhu, J. Nanopart. Res. 10 (2008) 59–67.
[36] M. Laferrière, R.E. Galian, V. Maurel, J.C. Scaiano, Chem. Commun. (2006) 257–259.